Density functional description of spin, lattice, and spin-lattice dynamics in antiferromagnetic and paramagnetic phases at finite temperatures

Davide Gambino [1], Oleksandr I. Malyi [2,*]

are corresponding projections of noncollinear local magnetic moment on the x, y, and z axes.

B. Calculation of the local spin motifs

The local spin motifs (LSMs) for atom i at time t are defined as

$$\mathrm{LSM}(i,t) \quad \frac{1}{N_{\mathrm{neighbors}}} \sum_{j\ 1}^{N_{\mathrm{neighbors}}} \hat{\boldsymbol{\mu}}_i(t) \quad \hat{\boldsymbol{\mu}}_j(t), \tag{4}$$

where $N_{\mathrm{neighbors}}$

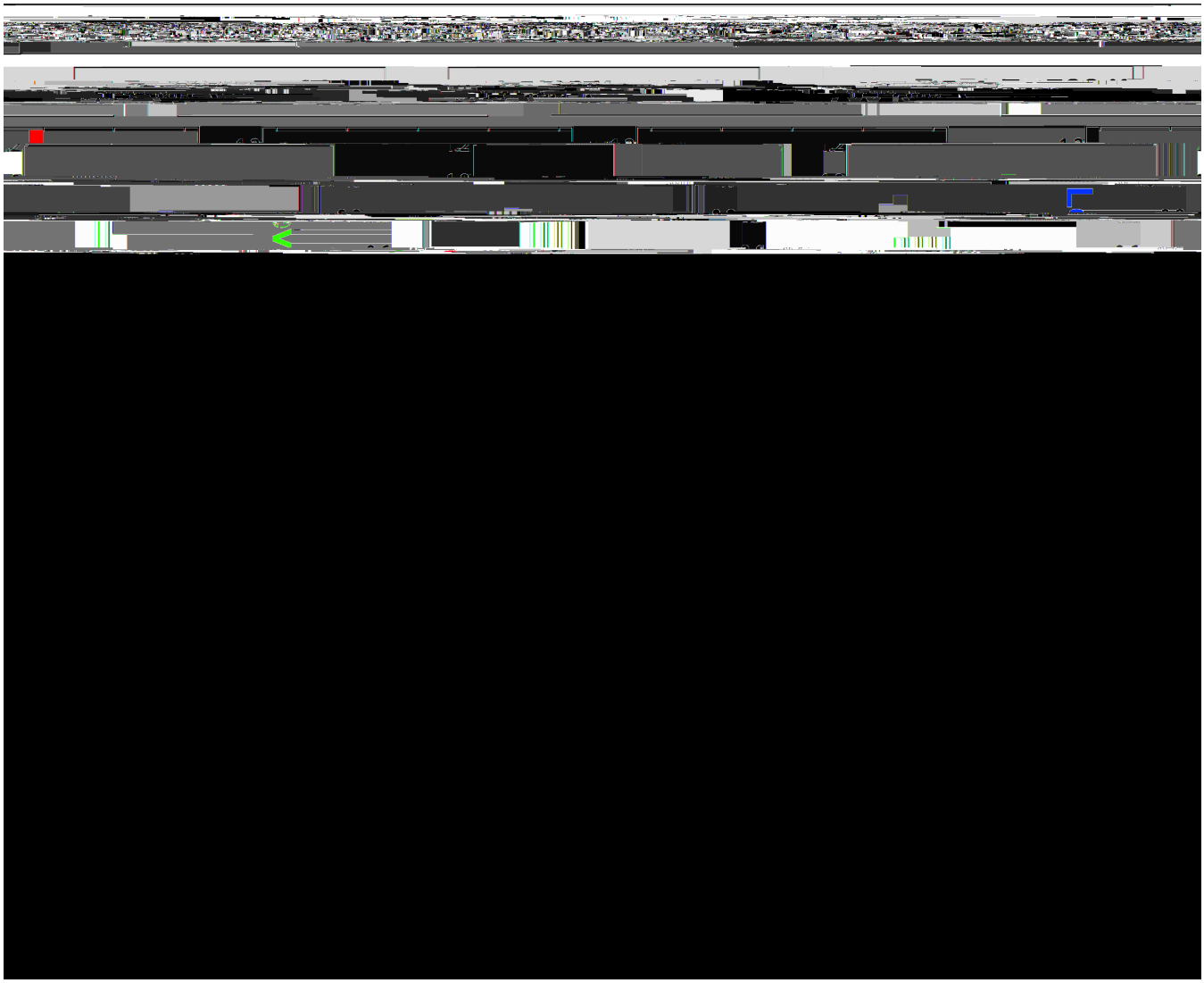

FIG. 4. Distribution of local spin motifs in the first coordination sphere for different temperatures and levels of spin-lattice dynamics.

failure of DFT, which has been claimed in many previous studies [43–45], is not fair.

Increase of temperature results in small changes in the distribution of magnetic moments, as shown in Fig. 3, which is both originated from the change of short-range spin order (discussed below) and from the different lattice constants for different temperatures. In Level II, the distribution is not as smooth as in the other two levels because only one spin configuration per temperature is employed here; therefore, each spin always maintains the same correlation with the neighboring spins, leading to a less homogenous fluctuation of the value of the local magnetic moment.

B. Distribution of LSMs

We perform detailed analysis of LSMs within the first and second coordination spheres calculated with Eq. (4). The results for different levels of spin-lattice dynamics summarized in Figs. 4 and 5 show that temperature results in a substantial broadening of the distribution of LSMs. This is especially visible for the first-coordination sphere (Fig. 4). The analysis

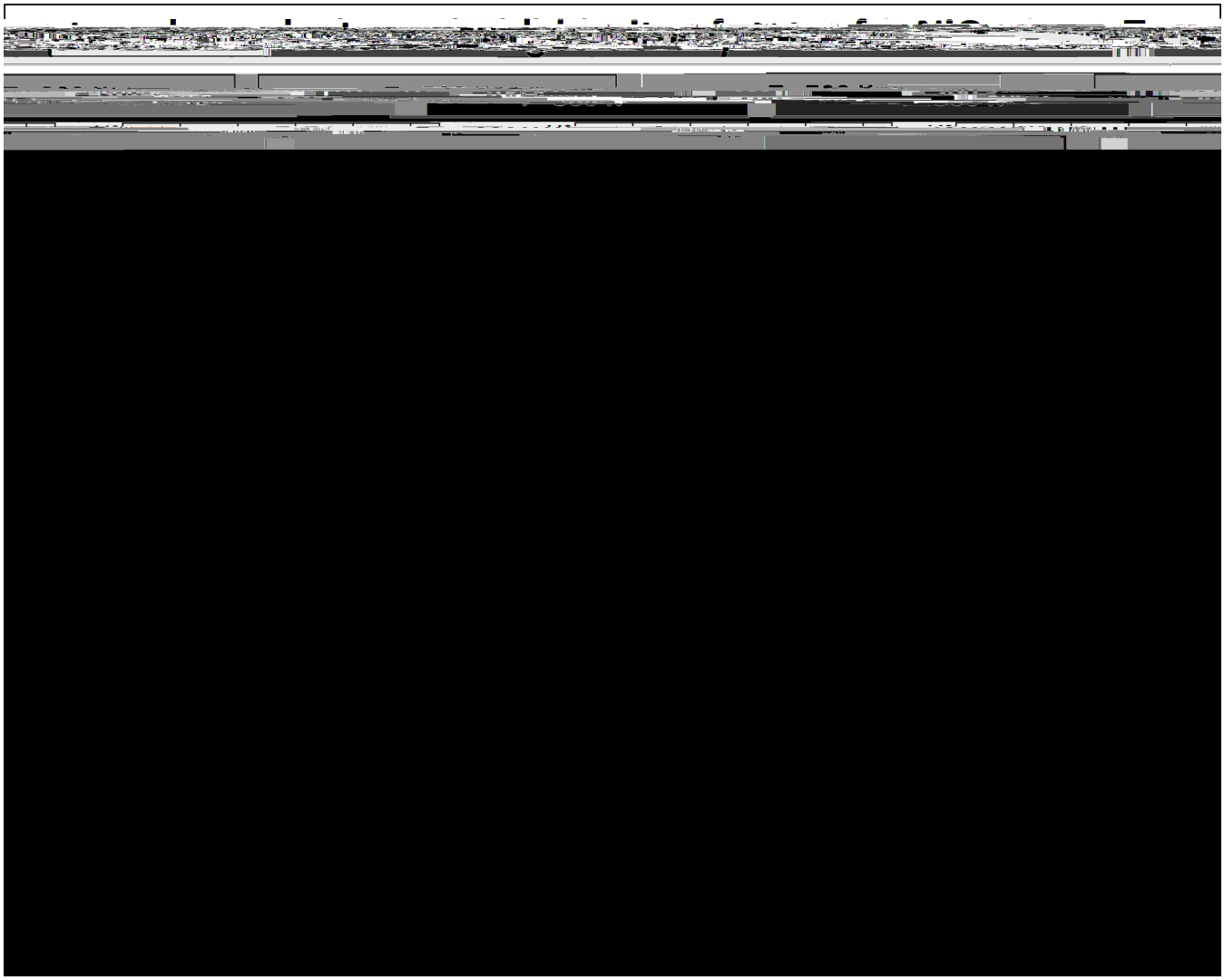

TABLE II. Bandgaps in energy and momentum, extracted from EBS with spectral function intensity > 0.1 Å eV ^{1} atom ^{1} for AFM, SQS, and Levels I, II, and III as a function of temperature. L-45%-Γ means that the band edge is along the L-Γ path having a distance to L 45% of the distance from L-Γ. All momenta are in the primitive Brillouin zone of single-cell rock salt NiO.

	Gap energy (eV)	Momentum (VBM to CBM)
AFM (T 0)	2.9	L-45%-Γ to Γ-40%-X
SQS-PM (inf. T)	2.42	L to Γ

	Level I		Level II		Level III	
T (K)	Gap energy (eV)	Momentum (VBM to CBM)	Gap energy (eV)	Momentum (VBM to CBM)	Gap energy (eV)	Momentum (VBM to CBM)
300	2.74	L-20%-Γ to Γ	2.6	L-38%-Γ to Γ	2.58	L-41%-Γ to Γ-45%-X
400	2.5	L-15%-Γ to Γ	2.44	L to Γ	2.50	L-38%-Γ to Γ
500	2.5	L to Γ	2.28	L to Γ	2.38	L-10%-Γ to Γ
600	2.38	L to Γ	2.12	L to Γ	2.30	L to Γ
700	2.42	L to Γ	2.08	L to Γ	2.18	L-26%-Γ to Γ

perature. This decrease is the smallest for Level I spin dynamics. This is not surprising, as Level I theory ignores the effect of thermal atomic vibration on electronic structure, which is known to reduce the bandgap energy in oxides [49] and can be seen by comparison of the results for Levels I and II theories. When comparing DOSs for Levels II and III spin-lattice dynamics, one clearly sees similarities in the electronic structures. The main difference here is only in relative intensities of the states at the band edges.

Comparing the present results with x-ray photoelectron spectroscopy measurements [50], we observe that inclusion of spin DOFs, together with the details of the employed PBE U functional, shows improvements with respect to previous LDA U results [51] co0 ga-.000b

coupled with AIMD to simulate a dynamically coupled spin and lattice state.

Our focus is on the electronic consequences of these levels of dynamics. We find that the effect of lattice vibrations and spin dynamics affects the EMPs of the system under investigation, and both effects should be considered at some level to obtain a full picture of the system. In Level III, we only observe minute differences from Level II in terms of DOS-derived bandgaps, but a somewhat larger difference is seen when evaluating the bandgap with the EBS-based method. This indicates that the electronic states in the vicinity of the band edges demonstrate some influence of the coupled dynamics even if the absolute band edge positions do not. Overall, however, we conclude that, for PM NiO, the important aspect in theoretical modeling is to consider disordered magnetism and lattice vibrations. The effect of their mutual dynamical coupling is not large on the properties studied here. Further investigations could be directed to properties such as phonon lifetimes, thermal conductivity, and other aspects where dynamical phenomena can have a larger impact.

ACKNOWLEDGMENTS

BA acknowledges funding from the Swedish Foundation for Strategic Research through the Future Research Leaders 6 program, Grant No. FFL 15-0290, from the Swedish Research Council (VR) through GrantG4.5(NiO,)-304.9(the)-3]TJ2019-0540345.83(couln Tc[(dynamics)-422.4)-409.902 48(absolute)-6

nickel oxide: disentangling phonons and magnons, Appl. Phys. Lett. **110**, 202406 (2017).

[21] E. Aytan, B. Debnath, F. Kargar, Y. Barlas, M. M. Lacerda, J. X. Li, R. K. Lake, J. Shi, and A. A. Balandin, Spin-phonon coupling in antiferromagnetic nickel oxide, Appl. Phys. Lett. **111**, 252402 (2017).

[22] S. M. Rezende, A. Azevedo, and R. L. Rodríguez-Suárez, Introduction to antiferromagnetic magnons, J. Appl. Phys. **126**, 151101 (2019).

[23] A. Lindmaa, R. Lizárraga, E. Holmström, I. A. Abrikosov, and B. Alling, Exchange interactions in paramagnetic amorphous and disordered crystalline CrN-based systems, Phys. Rev. B **88**, 054414 (2013).

[24] N. M. Rosengaard and B. Johansson, Finite-temperature study of itinerant ferromagnetism in Fe, Co, and Ni, Phys. Rev. B **55**, 14975 (1997).

[25] A. V Ruban, S. Khmelevskyi, P. Mohn, and B. Johansson, Temperature-induced longitudinal spin fluctuations in Fe and Ni, Phys. Rev. B **75**